DOI: 10.1002/ejic.201100119

Transformation of a Cu^{II} Thiazolo-1,2,4-triazine Derivative from a Metastable Coordination Network to a Monomer in Solution and Vapor Conditions

Akiko Hori,*[a] Takahiro Kikuchi,[a] Kumiko Miyamoto,[a] Takashi Okano,[b] Chihiro Kachi-Terajima,[c] and Hiroshi Sakaguchi[a]

Keywords: Coordination modes / Copper / Magnetic properties / Metastable compounds / Solvatochromism

Although mononuclear complexes were mainly obtained from Cu^{2+} ion and phenyl-, ethyl- or benzyl-substituted thiazolo-1,2,4-triazine derivatives, unique metastable orange–yellow crystals $[CuCl_2(\mathbf{3a})]_n$ (**5a**; Cu/**3a** = 1:1) with the phenyl-substituted derivative **3a** were obtained as a 1D coordination polymer through bis(μ-chloro) linkages in a 2-propanol solution. The crystals show dynamic and irreversible structural transformation into blue crystals of $[CuCl_2(\mathbf{3a})_2]$ (**6a**; Cu/**3a** = 1:2) not only in solution but also in vapor conditions. As **5a** and **6a** are ferromagnetic and paramagnetic, respectively, the transformation of **5a** was monitored by magnetic susceptibility measurements in the solid state, and χT of **5a** decreased according to the color change. The XRD pattern of **5a** also changed to a new aggregation state, ascribed to the disproportionation of the 1D network to form a mononuclear complex and a solvated metal ion in the crystalline state. This unusual 1D network is stabilized by intermolecular π-π stacking between the phenyl and the triazine moieties, and comparative studies of the ethyl and benzyl-substituted complexes show no polymeric structures. The coordination site of all the thiazolo-1,2,4-triazine derivatives in this work was found to be the imino nitrogen as a monodentate coordination site by X-ray crystallographic studies and DFT calculations.

Introduction

Thiourea and its derivatives have been widely investigated in order to understand their biological importance in compounds such as antagonists.[1–3] In particular, the development of the cyclization reaction of these species was inspired by synthetic interest[4–6] and regulation of the biological activity.[7,8] The condensed heterocyclic compounds with a thiourea framework, e.g. 1,2,4-triazine-3-thione and thiazolo-1,2,4-triazine derivatives, are targets because of the structural characteristics of the condensed donor sites (N, O, and S atoms) and their inhibitory activity against peroxidases containing Cu^{2+} ions.[9,10] However, the coordination mode of these heterocyclic compounds is unclear for two reasons: (i) few structural characterizations of the coordination complexes have been carried out[11,12] and (ii) dynamic exchange reactions of the coordination site occur between the multiple donor species depending on the external conditions.[13–15] Therefore, we examined some model compounds with Cu^{2+} ions to understand the coordination sites and to characterize the structure of the heterocyclic compounds.

The isomeric phenyl-substituted thiazolo-1,2,4-triazines, 3-phenyl-6,7-dihydro-4*H*-[1,3]thiazolo[2,3-*c*][1,2,4]triazin-4-one (**2a**) and 6-phenyl-2,3-dihydro-7*H*-[1,3]thiazolo[3,2-*b*]-[1,2,4]triazin-7-one (**3a**), were prepared from 6-phenyl-3-thioxo-3,4-dihydro-1,2,4-triazin-5(2*H*)-one (**1a**) (Scheme 1).[16] The ethyl- (**2b** and **3b**) and benzyl-substituted (**2c** and **3c**)

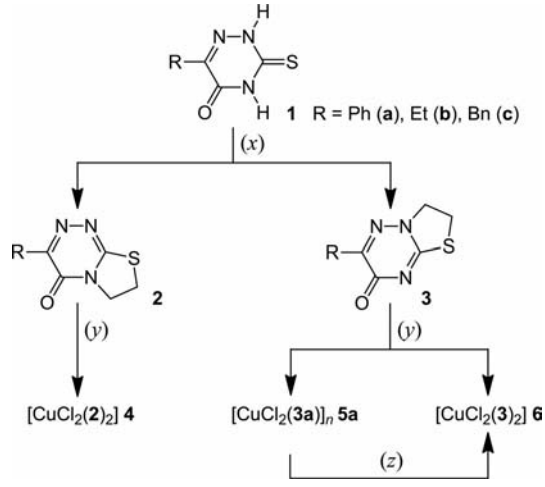

Scheme 1. Synthetic routes for the condensed heterocyclic rings and their complexation reactions, (x) dibromoethane, EtONa, (y) $CuCl_2{\cdot}2H_2O$, 2-propanol, (z) 2-propanol and/or water.

[a] Department of Chemistry, School of Science, Kitasato University,
1-15-1 Kitasato, Minami-ku, Sagamihara, Kanagawa 252-0373, Japan
Fax: +81-42-778-9953
E-mail: hori@kitasato-u.ac.jp
[b] Chemistry Laboratory, The Jikei University School of Medicine,
8-3-1 Kokuryo, Chofu, Tokyo 182-8570, Japan
[c] Department of Chemistry, Faculty of Science, Toho University,
2-2-1 Miyama, Funabashi, Chiba 274-8510, Japan
Supporting information for this article is available on the WWW under http://dx.doi.org/10.1002/ejic.200900119.

derivatives were also prepared in order to compare the coordination behavior with the phenyl derivatives. In this study, we successfully characterized the preferred coordination site of **4** and **6** by X-ray crystallographic studies and DFT calculations. Furthermore, vapochromism[17–27] of an unexpected metastable orange–yellow crystals of the coordination network (**5a**) and the thermodynamically stable blue monomer (**6a**) is discussed. The transformation of structures and related macroscopic properties, such as colors, magnetic moments, and crystal dimensions, between the different spin states induced by external manipulation is currently of interest.[28–30]

Results and Discussion

Synthesis and Crystal Structure of 4a

In the reaction of $CuCl_2{\cdot}2H_2O$ and **2a** in a 2-propanol solution, the mononuclear complex $[CuCl_2(\mathbf{2a})_2]$ (**4a**) ($CuCl_2$/**2a** = 1:2) was obtained as brown crystals in 76% yield. The result of the elemental analysis confirmed the purity of **4a**. Single crystals of **4a**·CH_2Cl_2 were obtained from a CH_2Cl_2 solution, which were suitable for X-ray crystallography. The crystal is monoclinic, *C*2/*c*, and the asymmetric unit contains two halves of the complex and one CH_2Cl_2 molecule. Both complex molecules in a unit cell are centrosymmetric and comprise one Cu^{2+} ion and two **2a** molecules. Hereafter, we only describe one complex molecule of **4a** (Figure 1) because of their similarity. Ligand **2a** is coordinated through the nitrogen N2 atom, which is different from the complexation of other thiourea condensed heterocyclic compounds.[11,12] The geometry around the Cu center is square planar; the Cu–N2 and Cu–Cl1 bond lengths are 1.9952(14) and 2.2332(4) Å, respectively. The intramolecular Cu···N1 and Cu···S1 distances are 2.8716(14) and 3.4039(5) Å, respectively. The torsion angle of Cl1–Cu–N2–C3 is 95.38(13)°, almost perpendicular between the aromatic plane and the $CuCl_2$ units. The closest intermolecular Cu···Cu distance is 5.9127(6) Å. Two phenyl moieties in **4a** show the same orientation in the crystal packing.

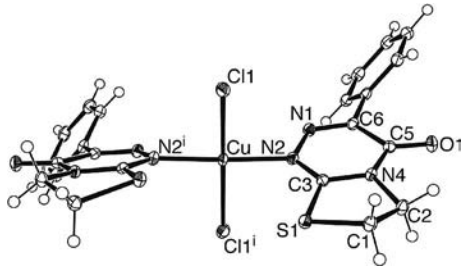

Figure 1. (a) ORTEP drawing of the molecular structure of **4a**·CH_2Cl_2 with 50% probability thermal ellipsoids at 100 K. The symmetry transformation used to generate equivalent atoms is i (–*x*, *y*, –*z* + 0.5).

Generally, it is difficult to predict the coordination site of such a multiheteroatomic molecule as **2a**. Geometry optimization by DFT (B3LYP/6-31G** for C, H, N, O, S, and Cl and LANL2DZ effective core basis set for Cu) molecular calculations for several complex structures of $[CuCl_2{\cdot}(\mathbf{2a})_2]$ revealed that the N2 complex (**4a**) is the most stable among the N1, N2, S1, and O1-coordinated structures. The optimized geometry of **4a** is slightly more stable (12.3 kJ mol^{-1}) than the N1-coordinated geometry. The S1 atom is strongly conjugated with the aromatic triazinone system in **2a** and coordination on the S1 atom seems to cause destabilization, i.e. the S1-coordinated form is 71.0 kJ mol^{-1} less stable than the **4a** form, and the optimized structure of the complex was considerably deformed from the square planer geometry. Interestingly, the S1-coordinated structure is also more unstable than the O1-coordinated imidate structure (ΔE = 40.2 kJ mol^{-1}).

Synthesis and Crystal Structures of 5 and 6

The reaction between $CuCl_2{\cdot}2H_2O$ and **3a** produced two products. Typically, a solution of $CuCl_2{\cdot}2H_2O$ in 2-propanol and **3a** dissolved in 2-propanol were combined at room temperature to produce orange–yellow and blue microcrystals as minor and major components, respectively. The yield of the orange–yellow product was less than 10% under these conditions. When the mixture was heated to around 70 °C or the complexation was conducted at a lower concentration (< 30 mM) at room temperature, only the blue crystals were obtained in almost quantitative yields. The blue product is thermodynamically more stable than the orange-yellow product. The result of the elemental analysis showed that the composition of the blue crystals **6a** is $CuCl_2$/**3a** = 1:2. When the reaction mixture in 2-propanol was maintained for several hours at room temperature, the orange–yellow microcrystals irreversibly disappeared into the solution and only the blue crystals remained. The orange–yellow product was not obtained from reactions with solvents such as methanol. From these results, we conclude that the orange–yellow product was kinetically precipitated as a metastable product under high concentration, low temperature, and excess-copper conditions. Thus, the orange–yellow microcrystals (**5a**) were quickly removed from the solution in order to avoid conversion into the blue crystals (**6a**). The result of the elemental analysis of **5a** indicated that the composition of the crystal is $CuCl_2$/**3a** = 1:1. Interestingly, vapochromism of **5a** was observed after filtration. The orange–yellow color irreversibly turned to bluish brown. Orange–yellow **5a** can be stored for several months under a dry atmosphere.

Single crystals of **5a** and **6a** suitable for X-ray crystallographic studies were obtained from a large-scale reaction of $CuCl_2{\cdot}2H_2O$ (10 mmol) and **3a** (10 mmol). The density difference (1.936 g cm^{-1} for **5a** and 1.730 g cm^{-1} for **6a**) helped to separate the two crystals in a solution of toluene/bromoform. A few crystalline particles were found with both orange–yellow and blue parts.

The asymmetric unit of **5a** (monoclinic, $P2_1/n$) comprises one Cu^{2+} ion, two chloride ions, and one **3a** molecule to give a 1D network through coordination bonds between the Cu^{2+} and Cl^- ions (Figure 2). The coordination site of **3a** is

the imino N4 atom. The geometry around the Cu is pseudo trigonal-bipyramidal; the Cu–N4, Cu–Cl1, Cu–Cl2, Cu–$Cl1^{ii}$ [symmetry code: (ii) $–x + 1, –y + 2, –z$] and Cu–$Cl2^{iii}$ [(iii) $–x + 2, –y + 2, –z$] bond lengths are 2.019(2), 2.3543(7), 2.3031(7), 2.2974(7), and 2.5761(7) Å, respectively. The Cl1–Cu–Cl2, N4–Cu–$Cl1^{ii}$, N4–Cu–$Cl2^{iii}$, and $Cl1^{ii}$–Cu–$Cl2^{iii}$ bond angles are 178.20(2), 147.01(6), 106.28(6), and 106.45(2)°, respectively. Thus, in the trigonal bipyramidal description, the apical sites are occupied by Cl1 and Cl2 with atoms N4, $Cl1^{ii}$, $Cl2^{iii}$, and Cu making up the equatorial plane. Two Cu^{2+} ions were linked by two $Cl^–$ ions to make a lozenge pattern; the Cu···Cu^{ii} and Cu···Cu^{iii} distances are 3.4618(8) and 3.6803(7) Å, respectively, and the bridging Cu–Cl1–Cu^{ii} and Cu–Cl2–Cu^{iii} bond angles are 96.17(3) and 97.77(2)°, respectively, forming the 1D network polymer along the *a* axis. The intramolecular Cu···O1 and Cu···S1 distances are 2.8371(18) and 3.6092(9) Å, respectively.

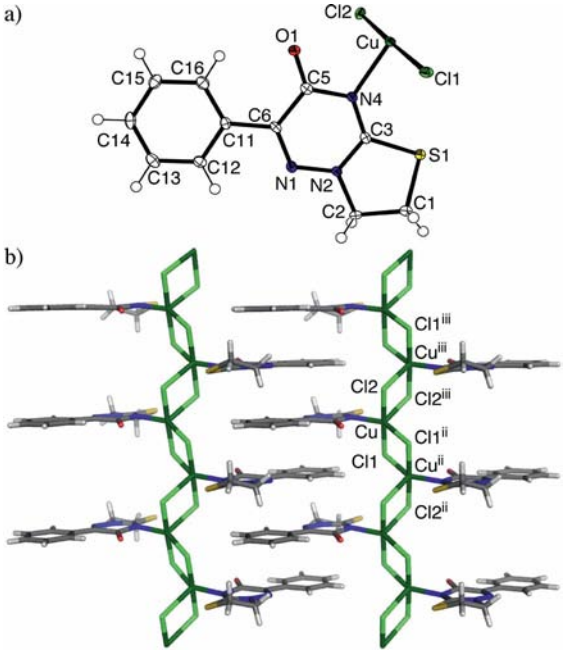

Figure 2. (a) Asymmetric unit of **5a** with 50% probability thermal ellipsoids at 100 K and (b) crystal packing views approximately along the *c* axis showing formation of the 1D network. The symmetry transformations used to generate equivalent atoms are ii ($–x + 1, –y + 2, –z$) and iii ($–x + 2, –y + 2, –z$).

The structural characteristics of bis(μ-chloro)Cu^{2+} complexes are summarized in Figure 3. The geometries of Cu^{2+} can be classified as square pyramidal **I** and trigonal bipyramidal **II** (Figure 3, a), which have been discussed in relation to their magnetic properties[14,15,31] and theoretical analysis[32] of the dimer. Several network types, **III**, **IV**, and **V** of bis(μ-chloro)Cu^{2+} complexes have been reported and the linear type **III** is well known; $(CuCl_2L_2)_n$[33,34] and $(Cu_2Cl_4L_2)_n$.[14,35] The ladder formation of **IV** and the zigzag formation of type **V** have also been reported $(CuCl_3L')_n$ (L′ = N_2H_5[36]) and $(CuCl_2L'')_n$ [L′′ = bipyridine[37] or di(2-pyridyl) ketone[38]], respectively, where two bidentate ligands L′′ are coordinated to each Cu^{2+} ion. In this work, the geometry around the Cu^{2+} center in **5a** is type **II**, and, to the best of our knowledge, the network formed is new and classified as type **VI** (Figure 3, b).[39]

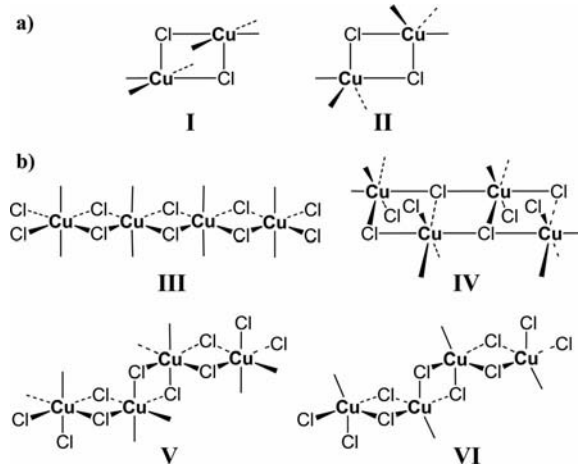

Figure 3. (a) Two common structures of bis(μ-chloro)Cu^{2+} dimers: square pyramidal (**I**) and trigonal bipyramidal (**II**); (b) four possible conformations of bis(μ-chloro)Cu^{2+} polymers: octahedral geometry with equatorial linear linkage (**III**), axial–equatorial ladder linkage (**IV**), axial–equatorial zigzag linkage (**V**), and five-coordinate zigzag linkage (**VI**).

The crystal structure of **6a** shows a typical mononuclear complex and the geometry around Cu is square planar (Figure 4). The crystal is triclinic, $P\bar{1}$, and the asymmetric unit contains half of the complex. The complex is centrosymmetric and comprises one Cu^{2+} ion and two **3a** molecules. The coordination site is also the N4 nitrogen atom. The Cu–N4 and Cu–Cl1 bond lengths are 2.0065(16) and 2.2486(6) Å, respectively. The intramolecular Cu···O1 and Cu···S1 distances are 2.9592(18) and 3.4427(16) Å, respectively. The torsion angle of Cl1–Cu–N4–C3 is 107.27(15)°, showing a twist between the aromatic plane and $CuCl_2$ units. The closest intermolecular Cu···Cu distance is 7.642(3) Å along the *a* axis.

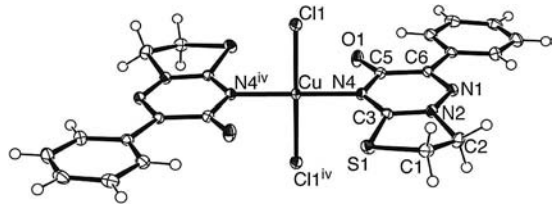

Figure 4. ORTEP drawing of the crystal structure of **6a** with 50% probability thermal ellipsoids at 100 K. Symmetry transformation used to generate equivalent atoms is iv ($–x + 2, –y + 1, –z + 1$).

The intermolecular stacking of the aromatic moieties of **6a** is similar to that of **5a**, which is shown in Figure 5. In **5a**, the electron-poor triazine ring N1/N2/C3/N4/C5/C6 (ring *A*) and electron-rich phenyl ring C11–C16 (ring *B*) closely interact with a head-to-tail arrangement of the molecules, showing a π-π interaction. The intermolecular distances between the two centroids of the rings, Cg*A*···CgB^{v} [(v) $–x + 2, –y + 1, –z$] is 3.4825(16) Å and the corresponding perpendicular distances of the rings Cg*A*···B^{v} is

3.2129(9) Å, where Cg*A* and Cg*B* are the centroid of the triazine ring and the phenyl ring, respectively (Figure 5, a). In **6a**, the triazine ring *A* and phenyl ring *B* also closely interact and the intermolecular distance between the two centroids of the rings, Cg*A*···Cg*B*^{vi} (–*x* + 1, –*y* + 1, –*z*) is 3.6520(19) Å and the corresponding perpendicular distance of the rings Cg*A*···*B*^{vi} is 3.2366(8) Å (Figure 5, b). Thus, the 1D network in **5a** is stabilized by π-π stacking. Compound **5a** is formed kinetically, when **3a** and Cu^{2+} ions are combined in high concentration. However, **5a** transforms into **6a** through a dissolution process because the trigonal bipyramidal conformation of the Cu^{2+} ion in **5a** is not stable as the square planar geometry of **6a**.

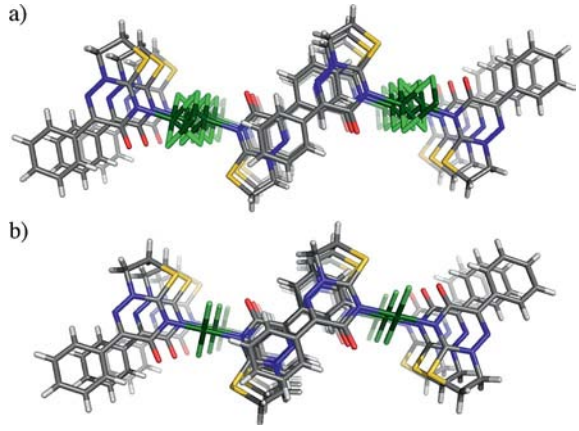

Figure 5. Crystal packing structures of (a) **5a** and (b) **6a** viewed along the *a* axis showing similar stacking between the ligands.

1D networks were not obtained for the ethyl- and benzyl-substituted compounds and only blue single crystals of **6b** and green single crystals of **6c** were obtained from **3b** and **3c**, respectively, using the same procedure for **3a**. This result also indicates that **5a** was obtained by the π-π stacking stabilization. The crystal structure information of **6b** and **6c** are summarized in the Supporting Information. These crystals are mononuclear Cu^{2+} complexes, whose coordination sites of the Cu^{2+} ions in **6b** and **6c** are the N4 nitrogen atoms. Selected bond lengths and angles are summarized in Table 1. No remarkable differences are observed around the metal centers of these three complexes; however, their crystal systems and the packing structures are different. The closest intermolecular Cu···Cu distances are 7.918(1) and 6.178(1) Å for **6b** and **6c**, respectively.

DFT calculations of $[CuCl_2 \cdot (\mathbf{3a})_2]$ also predicted the stability of the N4-coordinated structure. The optimized N4-coordinated **6a** is 54.7 kJ mol^{-1} more stable than the N1-coordinated structure, although **6a** is only 15.9 kJ mol^{-1} more stable than the O1-coordinated imidate structure. The triazinone moiety of the N1-coordinated structure is no longer planar, e.g. the torsion angles of N4–C5–C6–N1 in the optimized geometry are 10.6° and 9.7°. Thus, the aromacity of the triazinone is absent in this form. Again, coordination on the S1 atom seems to cause destabilization, i.e. the S1-coordinate form is 82.3 kJ mol^{-1} less stable than **6a**.

Table 1. Selected bond lengths [Å] and angles [°] of **6**.

Bond[a]	6a	6b	6c
Cu–Cl1	2.2486(6)	2.2602(4)	2.1942(9)
Cu–N4	2.0065(16)	1.9922(12)	2.036(2)
Cu···O1	2.9592(18)	2.8598(12)	3.098(2)
Cu···S1	3.4427(16)	3.5538(8)	3.4215(11)
Cl1···O1	3.358(2)	3.5737(14)	4.094(2)
Cl1···S1[a]	3.5979(16)	3.3287(8)	3.2528(12)
Cl1–Cu–N4	89.75(5)	90.18(4)	92.96(7)
N4–Cu–N4[a]	180	180	163.74(13)
Cu–N4–C3	124.98(13)	129.51(10)	123.10(19)
Cu–N4–C5	116.16(12)	111.90(10)	118.94(18)
Cl1–Cu–N4–C3	107.27(15)	91.99(13)	81.6(2)

[a] Corresponding intramolecular atoms on symmetric transformation.

Magnetic Properties and Vapochromism

Based on the difference between the Cu···Cu distances and geometries of **5a** and **6a**, we investigated their magnetic properties. Magnetic measurements for **5a** and **6a** were performed on polycrystalline samples in the temperature range of 2.0–300 K using an applied magnetic field of 10 kOe. The temperature dependence of χT for **5a** and **6a** are shown in Figure 6 (a).

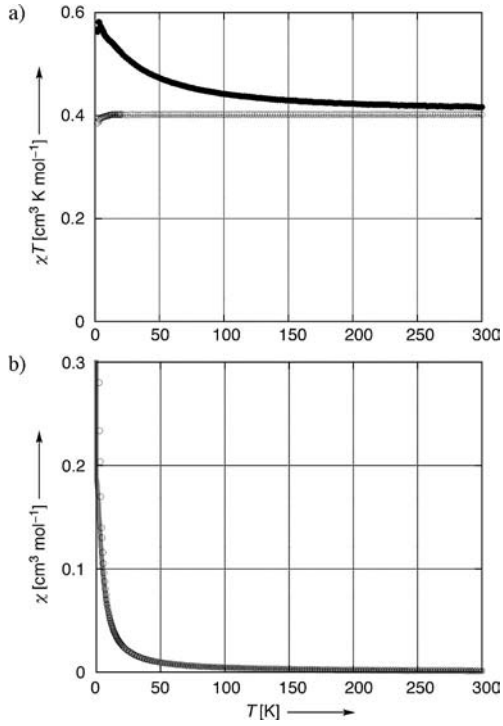

Figure 6. The temperature dependence of (a) χT measured on polycrystalline samples of **5a** (filled circles) and **6a** (open circles) at 10000 Oe and (b) χ for **5a** (open circles) with the best fitting curve (solid line).

For the 1D network **5a**, χT gradually increases with a temperature decrease, reaching a maximum of 0.58 cm^3 K mol^{-1} at 2.86 K, and then decreases. The magnetic susceptibility obeys the Curie–Weiss law above 50 K. The obtained Curie constant, C = 0.41 cm^3 K mol^{-1}, is slightly higher than the spin-only value (0.38 cm^3 K mol^{-1})

$$\chi_{chain} = \frac{Ng^2\mu_B{}^2}{4kT} \times \left[\frac{1.0 + 5.7979916x + 16.902653x^2 + 29.376885x^3 + 29.832959x^4 + 14.036918x^5}{1.0 + 2.7979916x + 7.0086780x^2 + 8.6538644x^3 + 4.5743114x^4} \right]^{2/3} \quad (1)$$

for one Cu^{2+}, S = 1/2 spin. The positive Weiss constant, θ = +8.0 K, is indicative of a ferromagnetic interaction between spin carriers. The 1D network **5a** is composed of two types of Cu–(Cl1)$_2$–Cu and Cu–(Cl2)$_2$–Cu bridges with different bond angles [96.17(3) and 97.77(2)°] and distances [Cu–Cl1 2.3543(7), Cu–Cl2 2.3031(7), Cu–Cl1^{ii} 2.2974(7), and Cu–Cl2^{iii} 2.5761(7) Å]. Although there are two different intrachain magnetic interactions in **5a** based on the structure data, we fitted the magnetic susceptibility data using the ferromagnetic S = 1/2 Heisenberg chain model,[40] assuming an average intrachain magnetic interaction (J_{av}) (see part a of Figure 5); $x = J/2kT$, see Equation (1). In order to take into account the interchain magnetic interaction, we used the following definition of the susceptibility in the mean-field approximation (J'), see Equation (2).[41]

$$\chi = \frac{\chi_{chain}}{1 - \frac{2zJ'}{Ng^2\mu_B^2}\chi_{chain}} \quad (2)$$

The best-fit results are obtained as J_{av}/k_B = +9.92(9) K, zJ'/k_B = –4.43(2) K and g_{av} = 2.100(1) using the data above 10 K in order to avoid some additional magnetic contributions such as weak magnetic interactions or magnetic anisotropy. Consequently, in **5a**, the intrachain magnetic coupling between the Cu^{2+} centers is ferromagnetic.

The magnetic coupling in dichloro-bridged Cu^{2+} complexes is very sensitive to the Cu–Cl–Cu angles, Cu–Cl distances, and distortions around the Cu^{2+} ions, dramatically varying from antiferromagnetic to ferromagnetic interactions with small structural changes.[42–47] The ferromagnetic coupling between the Cu^{2+} ions is also found in dichloro-bridged dimers[31,32,43–47] and chains[14,34] reported in the literature. In this work, two Cu–Cl–Cu angles of **5a** are in the middle of the range for bis(μ-chloro)Cu^{2+} dimer complexes,[31] which have the possibility of ferromagnetic and antiferromagnetic interactions in the intrachain structure. The four kinds of Cu–Cl bond lengths mentioned above show that Cl ion sites of the bridging center and the average bridging bond lengths are remarkably short compared with the dimers. For example, in the work on a dichloro-bridged dimer with a trigonal bipyramidal Cu^{2+} center (type II) of $[Cu(Et_3en)Cl_2]_2$,[31] the two Cu–Cl distances are 2.284(1) and 2.728(1) Å], and the Cu···Cu^{ii} and Cu···Cu^{iii} distances [3.4618(8) and 3.6803(7) Å] are short compared to those of bis(μ-chloro)Cu^{2+} dimers. In the network polymers, type III $(Cu_2Cl_4L_2)_n$ (L = 1-methylbenzotriazole)[14] is good example for comparison and is a molecular ferromagnet in which the chains are coupled antiferromagnetically: χT increases upon cooling at 20 K (0.62 cm^3 K mol^{-1}) and then decreases. In this complex, the Cu–Cl–Cu bond angle is 95.6(1)° and the Cu–Cl bond lengths are short [2.261(1) and 2.534(1) Å], giving a Cu···Cu distance of 3.556(1) Å. Hitherto, no magnetic characterization has been peformed on compounds with a zigzag orientation (type V and VI). The results for **5a** at around 2 K show an antiferromagnetic interaction, which is probably due to the interchain magnetic interaction because of the π-π stacking with relatively short C···C distances between the ligands of neighboring chains (ca. 3.25 Å).

Conversely, χT of the mononuclear complex **6a** remains almost constant over the entire temperature range. The plot of $1/\chi$ vs. T is described well by the Curie law above 2.0 K with the values of C = 0.40 cm^3 K mol^{-1}, which is also slightly higher than the theoretical spin-only value of 0.38 cm^3 K mol^{-1}, assuming an average g = 2.0 for one Cu^{2+} (S = 1/2) ion. This indicates that the intermolecular magnetic interactions are almost negligible in **6a**. Although the mononuclear molecules of **6a** exhibit π-π stacking (ca. 3.3 Å) between ligands, the Cu ions are magnetically isolated from each other.

The color of the orange–yellow powder **5a** (and single crystals) changed to bluish brown after filtration. This change was irreversible and very sensitive to moisture. Thus, we monitored the color change of **5a** by powder XRD patterns and magnetic measurements. The XRD clearly showed the orange–yellow powder to be **5a** (Figure 7, a and b). The powder was then kept under vapor conditions of water and/or 2-propanol, and the color

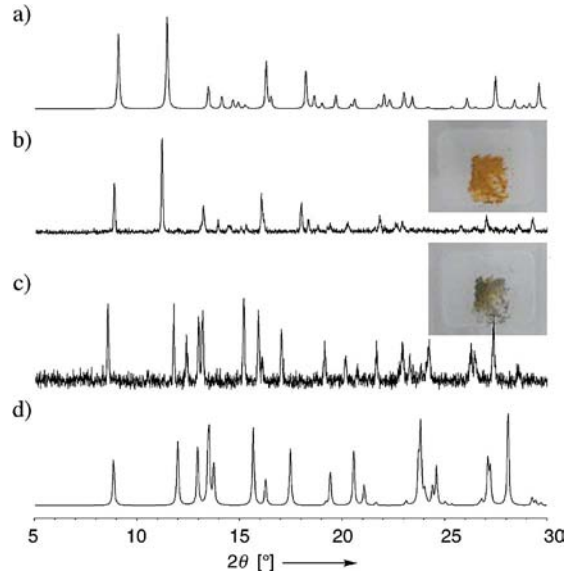

Figure 7. Powder X-ray pattern of (a) simulated pattern of the single crystal **5a**, (b) orange–yellow powder, (c) after the color change from the orange–yellow powder, and (d) simulated pattern of the single crystal **6a**.

changed to bluish brown. The XRD patterns of the powder dramatically changed (Figure 7, c). The peaks from **5a** disappeared and new weak and complicated peaks were observed, which were also different to **6a** (Figure 7, d). The ferromagnetic interaction of **5a** also decreased with the color change. Generally, the vapochromism is mainly induced due to two reasons: (i) a coordination exchange reaction between the metal and the solvents[15–18] and (ii) a change in the crystal packing due to inclusion of solvents.[19–25] In this case, we suggest that a dynamic disproportionation reaction of **5a** ($CuCl_2$/**3a** = 1:1) occurred and produced a new aggregation state composed of the mononuclear complex **6a** ($CuCl_2$/**3a** = 1:2) and the solvated metal ion in the solid. The orange–yellow powder **5a** is stable in a dry atmosphere after isolation from the solvent.

Conclusions

We have precisely characterized mono- and polynuclear coordination complexes with the thiazolo-1,2,4-triazine derivatives **2a** and **3a**. In the complexation reaction, the metastable 1D-network **5a** was obtained due to its lower solubility and kinetic stability, compared to the mononuclear complex **6a**. The orange product **5a** irreversibly transformed to the blue product **6a**. This color change is also observed in the powder samples; XRD studies show that the dynamic transformation between the complexes occurs in the solid state. The unexpected kinetic product was obtained and characterized because of the stabilization through π-π stacking between phenyl and triazine moieties. Both of the coordination sites with Cu^{2+} ions were proved to be the N imino donor through a single coordination bond. These results are important because several cases of multiple donor species in biological systems are assumed to be polydentate with predominantly S donors. These results also indicate that complicated coordination systems can be designed using multiple donor ligands. Controlling the coordination behavior by external conditions will be further investigated.

Experimental Section

General: All chemicals were of reagent grade and used without further purification. Ligands, **2** and **3**, were prepared as previously reported.[16] ^{1}H NMR spectra were recorded with a Bruker DRX600 spectrometer. The infrared spectra were recorded with a Shimadzu IR 8400s using a KBr disk. The melting points were determined with a Yanako MP-500D melting point apparatus. The elemental analysis of C, H, and N was performed with a Perkin–Elmer PE2400 analyzer. The DFT calculation using B3LYP/6-31G** (C, H, N, O, S, and Cl) and LANL2DZ (Cu) was performed using Spartan ′06 for Linux[48] on a home-made dual-core-CPU Linux machine. The magnetic susceptibility measurements were performed using a Quantum Design SQUID magnetometer MPMS-XL. DC (direct current) data were collected in the range from 2.0 to 300 K with an applied field of 10 kOe. The measurements were performed on polycrystalline samples that were wrapped in a Kapton sheet and fixed in a glass holder. The experimental data were corrected for trace background values of the sample holder and Kapton sheet, and for the sample's diamagnetic contribution calculated from Pascal constants.

Preparation and Physical Properties

[$CuCl_2$(2a)$_2$] (4a): 2-Propanol solutions of $CuCl_2{\cdot}2H_2O$ (43 mg, 0.25 mmol) and **2a** (58 mg, 0.25 mmol) were combined at room temperature to give brown microcystals; yield 76%; m.p. 201–202 °C. IR (KBr disk): $\tilde{\nu}$ = 1689, 1545, 1501, 1478, 1456, 1443, 1397, 1339, 1302, 1254, 795, 760, 694, 642 cm^{-1}. Elemental analysis: Calcd for $C_{22}H_{18}Cl_2CuN_6O_2S_2$ (%): C 44.26, H 3.04, N 14.08; found C 44.32, H 3.16, N 13.96. Crystallization was performed in a CH_2Cl_2/MeOH mixture to give dark blue plate crystals **4a**·CH_2Cl_2 suitable for X-ray crystallography.

[$CuCl_2$(3a)]$_n$ (5a): 2-Propanol solutions (5 mL) of $CuCl_2{\cdot}2H_2O$ (86 mg, 0.50 mmol) and **3a** (58 mg, 0.25 mmol) were combined at room temperature to give an orange–yellow powder of **5a** and a dark blue powder of **6a** as a mixture. This reaction is sensitive to external conditions. The purity of **5a** was examined each time by elemental analysis and the highest purity precipitates were used for further physical measurements; m.p. > 270 °C (dec). IR (KBr disk): $\tilde{\nu}$ = 1667, 1545, 1478, 1418, 1310, 1254, 1111, 806, 694 cm^{-1}. Elemental analysis: Calcd for $C_{11}H_9Cl_2CuN_3OS$ (%): C 36.12, H 2.48, N 11.49; found C 36.68, H 2.70, N 11.47. A higher concentration and a large amount of the starting materials unexpectedly produced a few orange–yellow block crystals. These crystals also disappeared in solution, and the blue crystals grew.

[$CuCl_2$(3a)$_2$] (6a): Complex **6a** was obtained as dark blue block crystals in the same reaction of **5a**; yield 93%; m.p. 243–244 °C. IR (KBr disk): $\tilde{\nu}$ = 1668, 1551, 1495, 1481, 1460, 1418, 1310, 1267, 1113, 806, 766, 696, 532 cm^{-1}. $C_{22}H_{18}Cl_2CuN_6O_2S_2$ (596.55): calcd. C 44.26, H 3.04, N 14.08; found C 44.21, H 3.02, N 13.97.

[$CuCl_2$(3b)$_2$] (6b): This was obtained as blue prismatic crystals using the same procedure as **6a** with **3b**; yield 76%; m.p. 198–200 °C. IR (KBr disk, cm^{-1}): $\tilde{\nu}$ = 1666, 1578, 1514, 1468, 1427, 1319, 1227, 1132, 453 cm^{-1}. $C_{14}H_{18}Cl_2CuN_6O_2S_2$ (500.55): calcd. C 33.57, H 3.62, N 16.78; found C 33.78, H 3.58, N 16.77.

[$CuCl_2$(3c)$_2$] (6c): This was obtained as green block crystals using the same procedure as **6a** with **3c**; yield 80%; m.p. 162–163 °C. IR (KBr disk, cm^{-1}): $\tilde{\nu}$ = 1661, 1576, 1487, 1439, 1425, 1418, 1242, 745, 698 cm^{-1}. $C_{24}H_{22}Cl_2CuN_6O_2S_2$ (624.58): calcd. C 46.12, H 3.55, N 13.45; found C 46.50, H 3.61, N 13.40.

X-ray Crystallography: Single crystal X-ray structures were determined with a Bruker SMART APEX CCD diffractometer with graphite monochrometer Mo-K_α (λ = 0.71073 Å) generated at 50 kV and 35 mA. All crystals were coated by paraton-N and were measured at 100 K. For all compounds, cell refinement and reduction were performed by using Bruker SAINT program, the structure solution was by using SHELXS97, the refinement was by SHELXL97.[49] All non-hydrogen atoms were refined anisotropically unless otherwise stated. H atoms attached to C atoms were constrained at idealized positions and refined riding on their carrier atoms, with aromatic, methylene, and methyl C–H distances of 0.95, 0.98, and 0.99 Å, respectively, and with Uiso(H) = 1.2 Ueq(C). The crystal data are summarized in Table 2. Powder XRD studies were curried out at room temp. using an M03XHF22 diffractometer (Mac Science) with Cu-K_α radiation (λ = 1.5418 Å).

CCDC-787916 (for **4a**·CH_2Cl_2), -787917 (for **5a**), -787918 (for **6a**), -787919 (for **6b**), and -787920 (for **6c**) contain the supplementary crystallographic data for this paper. These data can be obtained free of charge from The Cambridge Crystallographic Data Centre via www.ccdc.cam.ac.uk/data_request/cif.

Table 2. Crystal data for **4**–**6**.

	4a·CH_2Cl_2	**5a**	**6a**	**6b**	**6c**
Chemical formula	$C_{23}H_{20}Cl_4CuN_6O_2S_2$	$C_{11}H_9Cl_2CuN_3OS$	$C_{22}H_{18}Cl_2CuN_6O_2S_2$	$C_{14}H_{18}Cl_2CuN_6O_2S_2$	$C_{24}H_{22}Cl_2CuN_6O_2S_2$
M	681.94	365.73	597.01	500.93	625.07
T [K]	100	100	100	100	100
Crystal system	monoclinic	monoclinic	triclinic	monoclinic	tetragonal
Space group	$C2/c$	$P2_1/n$	$P\bar{1}$	$P2_1/c$	$I4_1/a$
a [Å]	30.887(3)	6.4900(11)	7.642(3)	8.5372(15)	14.526(3)
b [Å]	12.2113(10)	12.528(2)	8.152(3)	9.2054(17)	14.526(3)
c [Å]	14.9651(12)	15.436(3)	10.354(3)	12.885(2)	23.181(4)
α [°]	90	90	95.946 (3)	90	90
β [°]	106.609(1)	91.379(2)	100.979(3)	104.552(2)	90
γ [°]	90	90	112.710(3)	90	90
V [Å^3]	5408.9(8)	1254.7(4)	572.9(3)	980.1(3)	4891.5(16)
Z	8	4	1	2	8
D_c [g cm^{-3}]	1.675	1.936	1.730	1.697	1.697
U	1.393	2.324	1.405	1.623	1.320
F(000)	2760	732	303	510	2552
R_{int}	0.0220	0.0417	0.0158	0.0200	0.0307
Reflections measured	29926	13694	6322	10681	27290
Reflections independent	6168	2857	2483	2235	2802
GOF	1.116	1.034	1.190	1.247	1.094
$R[(I) > 2\sigma(I)]$	0.0244	0.0293	0.0223	0.0192	0.0438
$wR(F_o^2)$	0.0741	0.0666	0.0788	0.0760	0.1228

Supporting Information (see footnote on the first page of this article): Crystal structures for **6b** and **6c**, and DFT calculations for **4a** and **6a**.

Acknowledgments

This work was supported by a Kitasato University Research Grant for Young Researchers, and in part by a JST, PRESTO program.

[1] F. C. Odds, C. E. Webster, A. B. Abbott, *J. Antimicrob. Chemother.* **1984**, *14*, 105–114.
[2] D. H. Boschelli, D. T. Conner, D. A. Bornemeier, R. D. Dyer, J. A. Kennedy, P. J. Kuipers, G. C. Okonkwo, D. J. Schrier, C. D. Wright, *J. Med. Chem.* **1993**, *36*, 1802–1810.
[3] E. Bozo, G. Szilagyi, J. Janaka, *Arch. Pharm.* **1989**, *322*, 583–587.
[4] L. Fotouhi, R. Hekmatshoar, M. M. Heravi, S. Sadjadi, V. Rasmi, *Tetrahedron Lett.* **2008**, *49*, 6628–6630.
[5] A. Al-Etaibi, S. Makhseed, N. A. Al-Awadi, Y. A. Ibrahim, *Tetrahedron Lett.* **2005**, *46*, 31–35.
[6] J. Nyitrai, S. Békássy, K. Lempert, *Acta Chim. Acad. Sci. Hung.* **1967**, *53*, 311–314.
[7] R. K. Robins, *Chem. Eng. News* **1986**, *64*, 28.
[8] Y. A. Ibrahim, A. A. Abbas, A. H. M. Elwahy, *Carbohydr. Lett.* **1999**, *3*, 331–338.
[9] F. Arndt, W. Franke, W. Klose, J. Lorenz, K. Schwarz, *Liebigs Ann. Chem.* **1984**, 1302–1307.
[10] K. Miyamoto, H. Sakaguchi, S. Yoshii, H. Takayanagi, H. Ogura, Y. Iitaka, *Anal. Sci.* **1991**, *7*, 831–832.
[11] J. R. Anacona, A. Rodriguez, *Transition Met. Chem.* **2005**, *30*, 897–901.
[12] M. Ghassemzadeh, M. M. Pooramini, M. Tabatabaee, M. M. Heravi, B. Neumüller, *Z. Anorg. Allg. Chem.* **2004**, *630*, 403–406.
[13] K. Nomoto, S. Kume, H. Nishihara, *J. Am. Chem. Soc.* **2009**, *131*, 3830–3831.
[14] K. Skorda, T. C. Stamatatos, A. P. Vafiadis, A. T. Lithoxoidou, A. Terzis, S. P. Perlepes, J. Mrozinski, C. P. Raptopoulou, J. C. Plakatouras, E. G. Bakalbassis, *Inorg. Chim. Acta* **2005**, *358*, 565–582.
[15] D. B. Brown, J. W. Hall, H. M. Helis, E. G. Walton, D. J. Hodgson, W. E. Hatfield, *Inorg. Chem.* **1977**, *16*, 2675–2680.
[16] A. Hori, Y. Ishida, T. Kikuchi, K. Miyamoto, H. Sakaguchi, *Acta Crystallogr., Sect. C* **2009**, *65*, o593–o597.
[17] E. Cariati, X. Bu, P. C. Ford, *Chem. Mater.* **2000**, *12*, 3385–3391.
[18] J. Lefebvre, R. J. Batchelor, D. B. Leznoff, *J. Am. Chem. Soc.* **2004**, *126*, 16117–16125.
[19] A. Cingolani, S. Galli, N. Masciocchi, L. Pandolfo, C. Pettinari, A. Sironi, *J. Am. Chem. Soc.* **2005**, *127*, 6144–6146.
[20] N. Baho, D. Zargarian, *Inorg. Chem.* **2007**, *46*, 299–308.
[21] C. L. Exstrom, J. R. Sowa Jr, C. A. Daws, D. Janzen, K. R. Mann, *Chem. Mater.* **1995**, *7*, 15–17.
[22] M. Albrecht, M. Lutz, A. L. Spek, G. Van Koten, *Nature* **2000**, *406*, 970–974.
[23] C. E. Buss, K. R. Mann, *J. Am. Chem. Soc.* **2002**, *124*, 1031–1039.
[24] M. Kato, A. Omura, A. Toshikawa, S. Kishi, Y. Sugimoto, *Angew. Chem. Int. Ed.* **2002**, *41*, 3183–3185.
[25] T. J. Wadas, Q.-M. Wang, Y.-J. Kim, C. Flaschenreim, T. N. Blanton, R. Eisenberg, *J. Am. Chem. Soc.* **2004**, *126*, 16841–16849.
[26] C.-K. Koo, B. Lam, S.-K. Leung, M. H.-W. Lam, W.-Y. Wong, *J. Am. Chem. Soc.* **2006**, *128*, 16434–16435.
[27] R. Pattacini, C. Giansante, P. Ceroni, M. Maestri, P. Braunstein, *Chem. Eur. J.* **2007**, *13*, 10117–10128.
[28] P. D. Southonm, L. Liu, E. A. Fellows, D. J. Price, G. J. Halder, K. W. Chapman, B. Moubaraki, K. S. Murray, J.-F. Létard, C. J. Kepert, *J. Am. Chem. Soc.* **2009**, *131*, 10998–11009.
[29] M. Kepenekian, B. L. Guennic, V. Robert, *Phys. Rev. B* **2009**, *79*, 094428/1-094428/5.
[30] B. Li, R.-J. Wei, J. Tao, R.-B. Huang, L.-S. Zheng, Z. Zheng, *J. Am. Chem. Soc.* **2010**, *132*, 1558–1566.
[31] W. E. Marsh, K. C. Patel, W. E. Hatfield, D. J. Hodgson, *Inorg. Chem.* **1983**, *22*, 511–515.
[32] M. Rodríguez, A. Llobet, M. Corbella, *Polyhedron* **2000**, *19*, 2483–2491.
[33] B. Morison, *Acta Crystallogr., Sect. B* **1975**, *31*, 632–634.
[34] W. E. Estes, D. P. Gavel, W. E. Hatfield, D. J. Hodgson, *Inorg. Chem.* **1978**, *17*, 1415–1421.

[35] J. Reedijk, A. R. Siedle, R. A. Velapoldi, J. A. M. Van Hest, *Inorg. Chim. Acta* **1983**, *74*, 109–118.
[36] D. B. Brown, J. A. Donner, J. W. Hall, S. R. Wilson, R. B. Wilson, D. J. Hodgson, W. E. Hatfield, *Inorg. Chem.* **1979**, *18*, 2635–2641.
[37] M. T. Garland, D. Grandjean, E. Spodine, A. M. Atria, J. Manzur, *Acta Crystallogr., Sect. C* **1988**, *44*, 1209–1212.
[38] R. A. Mariezcurrena, A. W. Mombrú, L. Suescun, E. Kremer, R. Gonezález, *Acta Crystallogr., Sect. C* **1999**, *55*, 1989–1991.
[39] The relationship of the structures and the magnetic properties of Cl and O-linked network polymers has been investigated with the same types of structural classifications: a) H. Miyoshi, H. Ohya-Nishiguchi, Y. Deguchi, *Bull. Chem. Soc. Jpn.* **1972**, *45*, 682–684; b) D. D. Swank, C. P. Landee, R. D. Willett, *Phys. Rev. B* **1979**, *20*, 2154–2162.
[40] G. A. Baker, G. S. Rushbrooke, H. E. Gilbert, *Phys. Rev.* **1964**, *135*, A1272.
[41] C. J. O'Connor, *Prog. Inorg. Chem.* **1982**, *29*, 203.
[42] W. A. Alves, R. H. d. A. Santos, A. Paduan-Filho, C. C. Becerra, A. C. Borin, A. M. D. C. Ferreira, *Inorg. Chim. Acta* **2004**, *357*, 2269–2278.
[43] W. E. Estes, J. R. Wasson, J. W. Hall, W. E. Hatfield, *Inorg. Chem.* **1978**, *17*, 3657–3664.
[44] S. G. N. Roundhill, D. M. Roundhill, D. R. Bloomquist, C. Landee, R. D. Willett, D. M. Dooley, H. B. Gray, *Inorg. Chem.* **1979**, *18*, 831–835.
[45] W. E. Marsh, W. E. Hatfield, D. J. Hodgson, *Inorg. Chem.* **1982**, *21*, 2679–2684.
[46] R. Kapoor, A. Kataria, P. Kapoor, A. P. S. Pannu, M. S. Hundal, M. Corbella, *Polyhedron* **2007**, *26*, 5131–5138.
[47] S. Thakurta, P. Roy, G. Rosair, C. J. Gómez-García, E. Garribba, S. Mitra, *Polyhedron* **2009**, *28*, 695–702.
[48] *Spartan '06 for Linux*: Wavefunction, Inc. Irvine, CA, USA.
[49] G. M. Sheldrick, *Acta Crystallogr., Sect. A* **2008**, *64*, 112–122.
Received: February 4, 2011
Published Online: June 9, 2011

